OPTICAL PATH DIFFERENCE MODEL FOR THE VERY LARGE TELESCOPE INTERFEROMETER

Samuel Lévêque, Bertrand Koehler, Oskar von der Lühe

European Southern Observatory
Karl Schwarzschild Str.2
D-85748 Garching bei München

ABSTRACT

The optical path difference model (OPD model) determines where to position the delay lines in order to compensate for on-axis delay as seen from an astronomical object of known coordinates. This model is equivalent to a pointing model but applied to the interferometric delay. The objective is to reduce the time to search for fringes and to improve the delay lines blind tracking accuracy. This aspect is of prime importance not only when considering the overall operational efficiency of the interferometer but also its ability to quickly observe a set of program objects even after relocation of the auxiliary telescopes.

The optical path difference model is based on a precise knowledge of the interferometer configuration by including a set of calibration measurements. This paper describes the main characteristics of the model and includes the results of a simulation developed to fit telescope axis misalignments which contribute to optical path difference errors.

Keywords: Long baseline optical interferometry, Optical path compensation.

1. NEED FOR A GOOD ACCURACY ON FRINGE POSITION

In order to obtain fringes from an astronomical source with an interferometer consisting of several independent telescopes, the optical paths propagating from the object, through individual telescopes and towards a common beam combiner must be equalised. Thus, depending on the sky coordinates of the object, its diurnal motion, and the selected baseline of the interferometer, an internal delay must be continuously adjusted to balance the optical paths. This will be performed by moving delay lines along a 60m track.

In acquisition phase, the delay lines will be positioned according to a theoretical model where fringes are expected to be detected. A supplementary scan of the delay line may be necessary to detect fringes and then start a tracking procedure. Therefore, errors introduced in this predicted position will directly affect the time needed to acquire the interference signal.

A good accuracy on the fringe position will help (i) to have a quick access to a set of program stars even after reconfiguration of the auxiliary telescopes; (ii) to improve delay lines tracking accuracy especially in blind mode when no fringe tracking signal is available; (iii) to increase the overall operational efficiency of the interferometer.

2. CLASSICAL MODEL

2.1. Description

The fundamental equation which gives the OPD to be created as a function of time is given by:

$$OPD = \vec{S}.\vec{B} + OPD_{int} \qquad (1)$$

where

$\vec{S}$ is the unit vector pointing towards the object under study at a given time

$\vec{B}$ is the vector Baseline defined in 3 dimensional space.

$\vec{S}.\vec{B}$ is also known as vacuum delay. OPD_{int} is the internal OPD when the delay lines are at their mechanical reference positions. It corresponds to an offset of the Zero Path Difference position.

The ultimate accuracy on OPD is imposed by the star coordinates' accuracy. The external optical path difference can be written $OPD=B_p.\sin\theta$, where B_p is the projected baseline and θ the object's zenith distance. The angular position accuracy of an object taken from the Hipparcos catalogue will be 2mas . Thus an OPD error of ∂OPD =1 μm is expected for a star at zenith and a projected baseline of 100m. For sources taken from the FK5 catalogue, ∂OPD =25 μm in the same conditions. This numbers also apply for a 2° star switching. This paper does not take into account these errors.

Equation 1 relies on a good knowledge of the vector Baseline defined as the vector joining the intersection points of the altitude and azimuth axis of each telescope. The initial accuracy can be improved by astrometric calibration [1,2]. Starting from a set of reference stars $\vec{S}_i$ and an assumed vector baseline $\vec{B}_a$ the theoretical delays OPD_i, calculated with (1) are compared to the real fringe positions, $OPD_{r,i}$. A mean vector baseline $\vec{B}_m$ can be defined by writing

$$OPD_i - OPD_{r,i} = \vec{S}_i.(\vec{B}_a - \vec{B}_m) \qquad (2)$$

which can be solved for $\vec{B}_m$.

2.2. Limitations

The method illustrated by equation (2) has been used in existing interferometers operated with siderostats [1,2]. In these cases systematic OPD errors due to siderostat axis misalignments or run-outs were not taken into account. One relied on the intrinsic stability of the siderostats and further scanned the delay lines to acquire fringes.

When siderostats axes do not intersect, a mean pivot point can be defined [3] and a dedicated metrology monitors its movement. This is of importance when considering astrometric applications for which the knowledge of the baseline vector directly influences the final astrometric precision.

In the case of VLTI, axis misalignment and run-outs are expected to be equal to few 100 μm and the monitoring of a mean pivot point cannot be practically implemented. While sufficient accuracy may be obtained for fringe acquisition on bright stars, for which fringes position will be servoed during observation, axis misalignments may have a serious impact on the following two aspects. Firstly, on the blind tracking accuracy which requires an exact fringe position computation as a function of time. Secondly, on the VLTI astrometric mode.

It is therefore important to identify and model sources of systematic errors to improve the operation of VLTI. As an example, we studied the effect of telescope axes misalignements and run-outs on OPD errors.

3. INFLUENCE OF TELESCOPE'S AXIS MISALIGNMENT ON OPD ERRORS FOR VLTI

3.1. Configuration

Figure1 shows both azimuth and altitude axes whose mean separation is ε_m. Zenith and azimuth angles are respectively noted η and ζ. In order to simplify our discussion, we only considered circular runouts, R_{az} and R_{alt}. Runouts can further be described by phase angles φ_z and φ_a which define the instantaneous location of the two axes when $\eta=\zeta=0$. The projection of the altitude axis on the azimuth axis is defined by I_o when $\eta=\zeta=0$. This point is then considered to be linked to the telescope's tube and will move to a point $I(\eta,\zeta)$ when the telescope is pointing a given direction in the sky. Figure 2 illustrates the effect of the imperfections described above by showing the 3 dimensional displacement of $I(\eta,\zeta)$. The parameters were R_{az}=250 µm, R_{alt}=100 µm, ε_m =0, φ_z=10° and φ_a =20°.

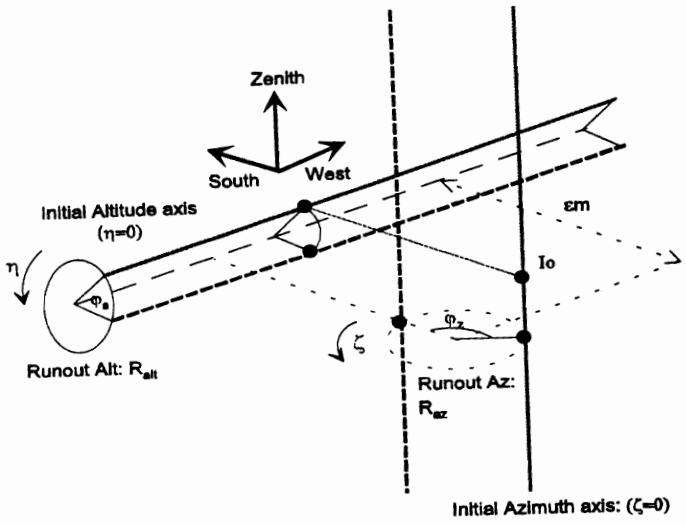

Figure 1: Telescope's axis configuration.

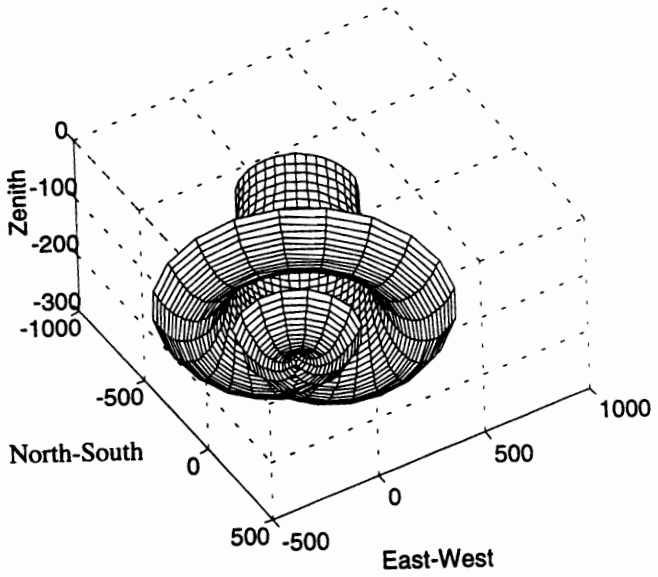

Figure 2: Displacement of $I(\eta,\zeta)$ in microns for $0<\zeta<360$ and $0<\eta<60$.

3.2. Computation of OPD errors

The quantity to be computed is defined as the OPD error, ε_{opd}, between a pair of telescopes which contains one telescope characterised by the misalignement described above and a pair of "perfect telescopes" (all parameters equal zero).

We used the concept of sensitivity matrix to compute the optical path disturbance induced by the 3D movement of each mirror of the telescope with respect to a referential linked to the ground.

In order to simplify our discussion, we considered the primary, secondary and tertiary mirrors as a rigid body linked to the telescope's tube. Similarly, the Coudé train mirrors were considered as a rigid body attached to the telescope's fork. Therefore, we studied, as a function of (η, ζ), the displacement of the tube and the fork due to axis misalignment, with respect to the referential [West, South, Zenith]. Equation 3 gives the OPD error as a function of (η,ζ) and is plotted figure3.

$$\varepsilon_{opd} =$$

$$[1\ \ 0\ \ -1]\begin{bmatrix}1 & 0 & 0\\ 0 & \cos\eta & -\sin\eta\\ 0 & \sin\eta & \cos\eta\end{bmatrix}\begin{bmatrix}-2\sin\frac{\zeta}{2}.\cos(\frac{\zeta}{2}+\varphi_z) & -2\sin 2\zeta.\sin(\frac{\eta}{2}+\varphi_a).\sin\frac{\eta}{2} & -\sin 2\zeta.(1-\cos 2\eta)\\ -2\sin\frac{\zeta}{2}.\sin(\frac{\zeta}{2}+\varphi_z) & 2\cos 2\zeta.\sin(\frac{\eta}{2}+\varphi_a).\sin\frac{\eta}{2} & \cos 2\zeta.(1-\cos 2\eta)\\ 0 & 2\sin\frac{\eta}{2}.\cos(\frac{\eta}{2}+\varphi_a) & \sin 2\eta\end{bmatrix}\begin{bmatrix}R_{az}\\ R_{alt}\\ \varepsilon_m - R_{az}.\cos\varphi_z - R_{alt}.\cos\varphi_a\end{bmatrix}$$

$$+\quad [-1\ \ 0\ \ 1]\begin{bmatrix}\cos\zeta & \sin\zeta & 0\\ -\sin\zeta & \cos\zeta & 0\\ 0 & 0 & 1\end{bmatrix}\begin{bmatrix}-2\sin\frac{\zeta}{2}.\cos(\frac{\zeta}{2}+\varphi_z) & 0 & 0\\ -2\sin\frac{\zeta}{2}.\sin(\frac{\zeta}{2}+\varphi_z) & 0 & 0\\ 0 & 0 & 0\end{bmatrix}\begin{bmatrix}R_{az}\\ R_{alt}\\ \varepsilon_m\end{bmatrix} \qquad (3)$$

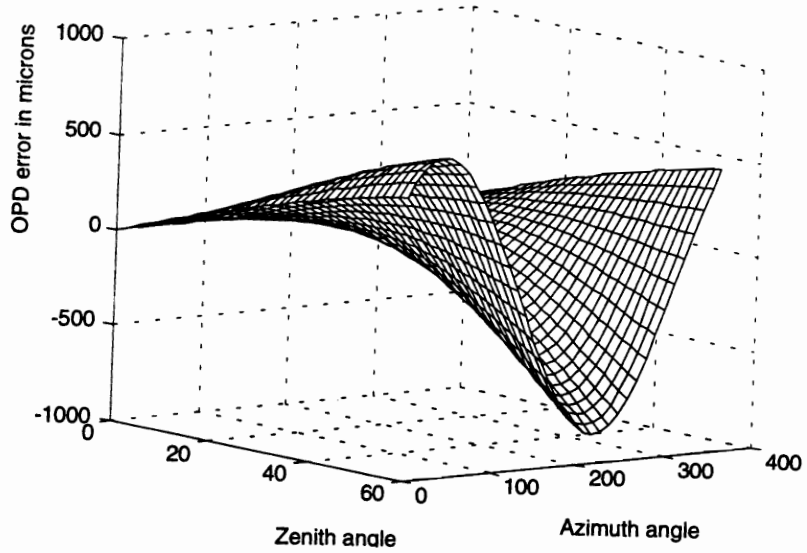

Figure 3: OPD error for $0<\zeta<360$ and $0<\eta<60$.

3.3. Consequences according to observing sequence

We considered 3 different scenarios, namely fringe acquisition, star switching and blind tracking. Fringe acquisition is the procedure followed to find the central fringe after pointing towards any object in the sky. Star switching is the action to blindly move the delay lines from a position where fringes are detected from a bright reference star to a position where fringes are expected to be detected from a nearby faint object. Finally blind tracking is an observing mode where tracking is performed on a faint object without any feedback from the fringe phase but according to theoretical laws.

Table 1 summarises the OPD errors obtained with the parameters of section 3.1. For fringe acquisition, the maximum OPD errors is directly given by Figure3. Then we looked at the derivatives as a function of zenith and azimuth angles. A two degree star switching represents the expected maximum angular separation between a bright reference source, used for fringe acquisition, and a program source observed in blind mode.

The OPD errors as a function of observing time is given by

$$\frac{\partial\varepsilon_{opd}}{\partial t} = \frac{\partial\varepsilon_{opd}}{\partial\eta}\cdot\frac{\partial\eta}{\partial t} + \cdot\frac{\partial\varepsilon_{opd}}{\partial\zeta}\cdot\frac{\partial\zeta}{\partial t}$$

where $d\eta/dt = -\omega_0 . \sin(\zeta) \cos(\phi)$ and $d\zeta/dt = -\omega_0 . [\sin(\phi) + 1/\tan(\eta) . \cos(\zeta) . \cos(\phi)]$.
ω_0 is the earth rotation rate (7.27.10-5 rad/s) and ϕ the site's latitude (-24° for Paranal).

This analysis shows that in the worst case, an OPD error equivalent to the expected 20µm rms atmospheric error will be reached only after 5min of blind observation.

Max. OPD error in fringe acquisition		$\partial\varepsilon_{opd}$ max=850 µm
Max. OPD error for a 2° switching		
altitude switching	$\frac{\partial\varepsilon_{opd}}{\partial\eta}$ max= 15.10^{-4}	$\partial\varepsilon_{opd}$ =50 µm
azimuth switching	$\frac{\partial\varepsilon_{opd}}{\partial\zeta}$ max=8.10^{-4}	$\partial\varepsilon_{opd}$ =30 µm
Blind mode tracking accuracy	$\frac{\partial\varepsilon_{opd}}{\partial t}$ max= **7.10^{-8} m/s**	after 5min $\partial\varepsilon_{opd}$ =20 µm

Table 1

3.4. Consequences for Astrometry

The angular separation between two stars is directly related to the optical path difference offset between their respective fringe packets. While tracking on a reference star of well known angular coordinates, the position of the program star's fringes is recorded from which the astrometric information is derived [1,5]. (η, ζ) are the coordinates of the reference star and $(\eta+\Delta\eta, \zeta+\Delta\zeta)$ those of the program source. $\Delta\eta$ and $\Delta\zeta$ are assumed to be small, 30 arcsec maximum. The angular star separation is determined from:

$$\Delta OPD_n = \vec{B} . (\vec{S}(\eta, \zeta) - \vec{S}(\eta+\Delta\eta, \zeta+\Delta\zeta)) \qquad (3)$$

Astrometric accuracy at the 10µarcsec level requires that the baseline shall be determined within 50µm [5]. The baseline defined as intersection point between axis cannot be practically measured with few tens of microns accuracy. The notion of instantaneous baseline as seen by the star must be used. Otherwise the ultimate astrometric accuracy will be limited to the amount of axis runouts and misalignment.

4. OPD MODEL FOR VLTI

The Optical Path Difference Model is part of the general OPD compensation problem whose objective is to adjust the delay line position to minimise the OPD rms error over various exposure times.

It computes a value of the OPD to be created by the delay lines as a function of time, in order to be as close as possible to the real fringe position which is affected by atmospheric, vibration and thermal effects. A fringe tracking control loop will be available when observing sufficiently bright sources to reduce atmospheric effects. Our contribution is to include terms for correction of systematic errors such as those presented in part 3.

We propose to consider the OPD model as the general telescope pointing model. Indeed, the telescope pointing model deals with errors on telescope axis and encoders which influence the pointing and tracking accuracy. By observing a set of reference stars, this model provides a two dimensional correction (altitude and azimuth) which finally reduces pointing errors from several arcmin to some arcsec [6].

By comparison, the OPD model will improve the acquisition and tracking accuracy by reducing the OPD errors. The time needed to acquire fringes with the OPD model can be seen as the time needed to lock on a star using a pointing model.

The parameters of the OPD model are:

- mean baseline coordinates: [Bx , By , Bz]
- internal optical path difference: OPDint
- residual source of systematic errors: for example [R_{az}, R_{alt}, ε_m, φ_a, φ_z ,...] which contributes to the OPD by the amount $E(\eta,\zeta)$.

Other terms such as axis wobble which influence the OPD error could also be implemented. All the parameters will be fitted to sky observations. For a set of calibration stars, the delay line metrology will measure the necessary OPD which has been created to centre fringes. Then an appropriate algorithm will determined all parameters in order to fit the measurements to the equation:

$$OPD(\eta,\zeta) = \vec{S}(\eta,\zeta).\vec{B}_m + OPD_{int} + E(\eta,\zeta) \qquad (4)$$

$E(\eta, \zeta)$ is a function of the parameters [P]=[R_{az} , R_{alt}, ε_m, φa, φ_z]. The coarse geometry of the array will provide a first guess of the baseline whereas the internal OPD will be measured from the Interferometric Laboratory to a retroreflector located on M2 or to a flat mirror located at the folded Nasmyth focus.

5. SIMULATION

5.1. Data flow

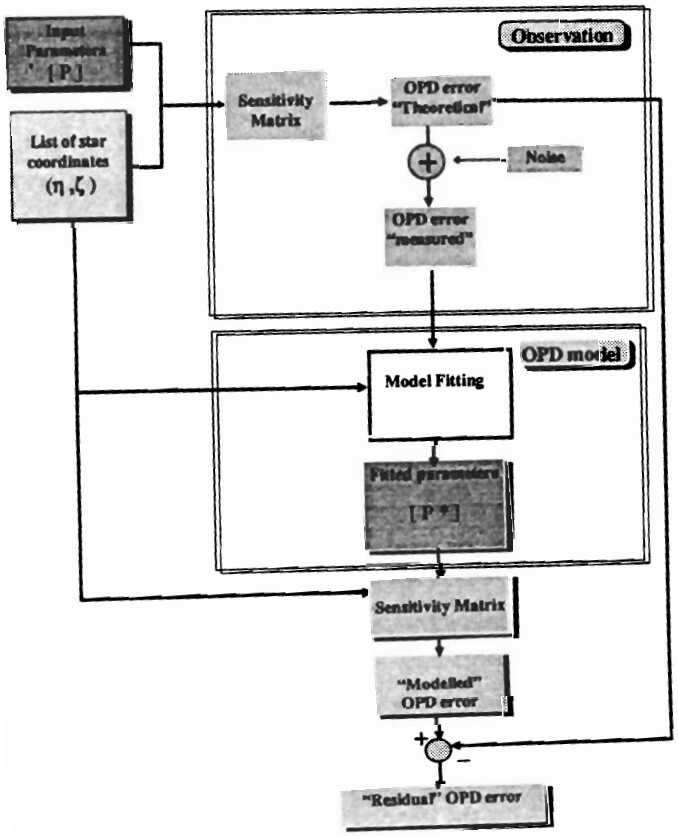

Figure 4: Simulation data flow

We performed a simulation to investigate how to determine the axis misaligment parameters from sky calibration and to assess the final OPD accuracy achievable.

First we selected from the FK5 catalogue a list of about 200 stars observable at a given date, equally distributed in the sky and with a maximum zenith angle equals to 60°.

Figure 4 shows the different steps followed to simulate a calibration run. Given a set of parameters, [P], and using equation (3), we calculated the "theoretical" OPD error that would occur by observing several calibration stars homogeneously picked up from the star list. This measure is degraded by atmospheric and delay line metrology noise which is expected to be around 20µm rms. Thus, we obtained a file containing calibration star coordinates and "measured" OPD error. Secondly, based on a "simplex" algorithm, we estimated a set of parameters [P*] that best fits the measurements.

In order to evaluate the fitting performances, we used again the initial 200 stars. For these stars, we compared the "modelled" OPD error, using [P*], to the theoretical OPD error which initially occurred with [P]. The difference between these two quantities is the "residual" OPD error which is an indication of the final accuracy of the OPD model fitting process.

Finally the effect of the number of calibration stars on the final OPD accuracy has been studied.

5.2. Results

Figure 5 presents the residual OPD error after correction computed for the initial list of stars sorted by azimuth. Three cases are displayed. First, the curve with the maximum amplitude shows OPD error when no attempt to fit telescope misalignment is undertaken. Then the number of calibration stars is increased to respectively 10 and 20.

Figure 6 shows the mean and rms residual OPD error as a function of the number of calibration stars used to evaluate the parameters. In this way, we found that the optimum number of calibration stars is between 10 and 20.

The input parameters were R_{az}=100μm , R_{alt}=200μm, ε_m=300μm, φ_z =10° and φ_a =20° which represent realistic values. Starting with a mean OPD error of 150±100 μm, the application of the OPD model with 20 calibration stars reduced errors to 3±3μm rms which lead to a gain of about 50.

We also implemented and tested a genetic algorithm but it did not perform with sufficient accuracy. A possible reason is that the maximisation process involved in the fitting of the parameters did not suffer from local minima. R_{alt} and φ_a were always difficult to guess because the possible observed altitude angles are restricted between 30 and 90°.

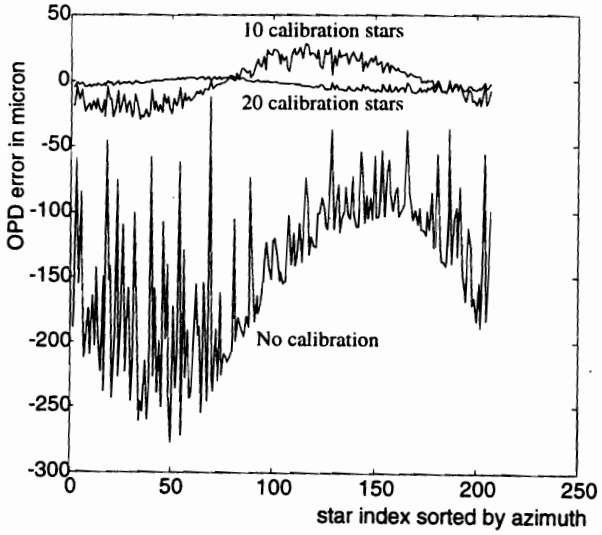

Figure 5: "residual" OPD error as a function of the initial 200 stars.

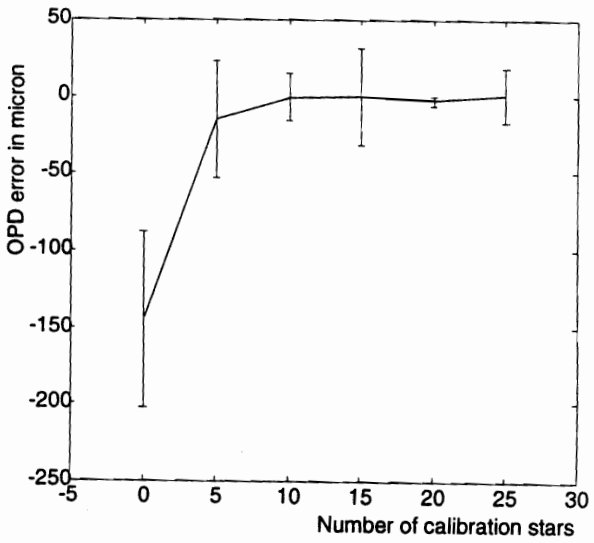

Figure 6: mean "residual" OPD error for the initial 200 stars, as a function of the number of calibration stars.

6. CONCLUSION

In order to improve the performance of the VLTI blind mode (i.e. when no fringe tracking signal is available) and its potential astrometric capability, we propose to implement an Optical Path Difference model, similar to a telescope pointing model. The OPD model will allow to trace and reduce systematic OPD errors. As an example, the influence of axis misalignment on OPD errors were presented. In this case, a simulation of a possible OPD model scheme has shown that after evaluation of the misaligments with 20 calibration stars, the OPD error was reduced by a factor 50 and brought down to a mean value of 3μm.

7. REFERENCES

[1] C.A Hummel et al. , "Four years of astrometric measurements with the Mark III optical interferometer", The astronomical journal, vol.108, number 1, p.326, July 1994.
[2] D.J. Hutter, " Siderostat/site metrology system for the USNO Astrometric optical Interferometer", proceedings ESO conference on high resolution imaging by interferometry II, Garching bei Muenchen, 1991.
[3] O. von der Lühe, A.Quirrenbach , "Calibration of the VLT interferometer", ESO/ST-ECF workshop, Calibrating and understanding HST and ESO instruments, ESO Garching 25-28 april 1995.
[4] M. Cullum, "VLT specification, basic telescope definitions", ESO report VLT-SPE-ESO-10000-0016.
[5] O. von der Lühe, A. Quirrenbach, B. Koehler, "Narrow-Angle Astrometry with the VLT Interferometer", Proceedings of the ESO Workshop Science with the VLT, 28 June-1July 1994, Springer Verlag 1995.
[6] P.T. Wallace, "TPOINT, a telescope pointing analysis system", TPOINT software,19 Sutton Wick Lane, Drayton, OX14 4HH, UK.